Imaging mid-ocean ridge transitions with satellite gravity

Christopher Small
David T. Sandwell
Scripps Institution of Oceanography, La Jolla, California 92093

ABSTRACT

Gravity maps derived from satellite altimeter measurements provide unprecedented medium-resolution coverage of sparsely surveyed mid-ocean ridges in the southern oceans. A spectral analysis of 76 000 km of coincident shipboard and satellite gravity measurements shows that satellite altimeters can accurately resolve features with half-wavelengths as short as 13 km. The coverage and resolution of these gravity data allow us to determine accurately both the location of poorly charted ridge axes and the variation in axial anomaly character along the ridge axis, although their detailed morphology is not resolved. The results of this study support earlier studies that showed a transition from spreading-rate–dependent axial gravity lows to rate-independent axial highs with increasing spreading rate. Four such transitions are imaged on the Southeast Indian Ridge and Pacific Antarctic Ridge. We expect that these transitions are the result of a temperature-sensitive threshold phenomenon and may be influenced by nearby hot spots.

INTRODUCTION

The radically different morphology of fast- and slow-spreading mid-ocean ridges is one of the earliest observations of seafloor structure, but it has yet to be fully understood. Heezen (1960) and Menard (1960) observed that the slow-spreading Mid-Atlantic Ridge is marked by a 1–3-km-deep axial valley with flanking rift valley mountains and rough topography, whereas the faster spreading East Pacific Rise generally consists of a more continuous axial ridge with smoother flanking topography (Fig. 1). The fast- and slow-spreading end members of the continuous mid-ocean ridge system have been studied extensively (e.g., Macdonald, 1986; Lonsdale, 1989) but the more remote intermediate-rate ridges have been largely overlooked.

Satellite altimeters provide medium-resolution gravity data with nearly complete coverage of the global mid-ocean ridge system. Recently declassified Geosat Geodetic Mission altimeter data provide exceptionally dense spatial coverage (2–4 km track spacing) of the oceanic areas south of lat 30°S. These remote southern oceans contain a significant part of the global mid-ocean ridge system and have not been adequately surveyed since the introduction of multi–narrow-beam echosounders such as Seabeam, Hydrosweep, and Seabeam 2000. In this paper we discuss the nature of morphologic transitions on intermediate-spreading-rate ridges in the southern oceans and the constraints offered by satellite gravity data.

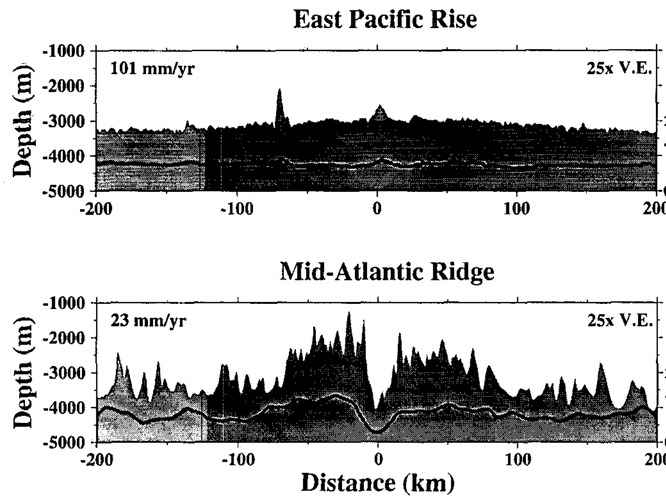

Figure 1. Typical ridge-axis bathymetry and gravity anomalies (heavy line) across fast- and slow-spreading mid-ocean ridges.

SATELLITE GRAVITY

Because the height of the ocean's surface above a reference corresponds to a gravitational equipotential, sea surface elevations measured by satellite altimeters may be used to produce geoid (Rapp, 1983) and gravity (Haxby et al., 1983) maps of the world's ocean basins. The method used to construct the gravity grids, described in detail by Sandwell (1992), allows data from the Seasat, Geosat, and ERS-1 satellite missions to be combined to give maximum spatial coverage. In addition, the very dense spatial coverage of recently declassified Geosat GM data allows much higher resolution of the gravity field in the areas south of 30°S.

Although satellite altimeters have lower spatial resolution than shipboard gravimeters, satellites provide superior areal coverage and are able to resolve large- and intermediate-scale features of the marine gravity field. Shipboard and satellite gravity profiles are shown for comparison in Figure 2A. The solid line shows the free-air anomaly as measured by a gravimeter on the USS *Eltanin* in the Indian Ocean in 1971. The dashed line represents the free-air anomalies interpolated from the satellite gravity grid along the same profile. It is apparent that the satellite data accurately resolve the salient features seen in the shipboard profile but do not resolve the shortest wavelength, low-amplitude features. Before using the satellite gravity data for detailed studies, it is necessary to quantify this agreement.

In order to quantitatively compare the resolution of the two types of gravity measurements, we performed a spectral analysis on 76 000 km of coincident shipboard and satellite measurements in the southern oceans. Although we used the highest quality data available, most of the data in the southern oceans were collected before Global Positioning Satellite navigation was available and may con-

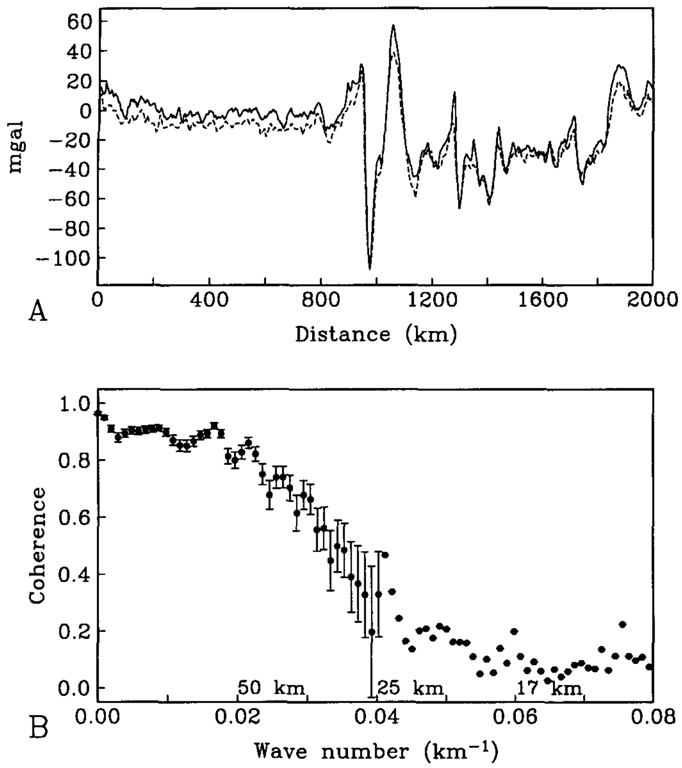

Figure 2. Comparison of coincident satellite and shipboard free-air gravity measurements. A: On profiles, satellite data (dashed line) resolve all but smallest features seen in ship data (solid line). Thickened line shows location of profile in Figure 3 (at ~90°E). B: Spectral coherence of 76 000 km of coincident ship and satellite gravity measurements shows very high agreement (>0.5) for anomalies with wavelengths longer than ~35 km.

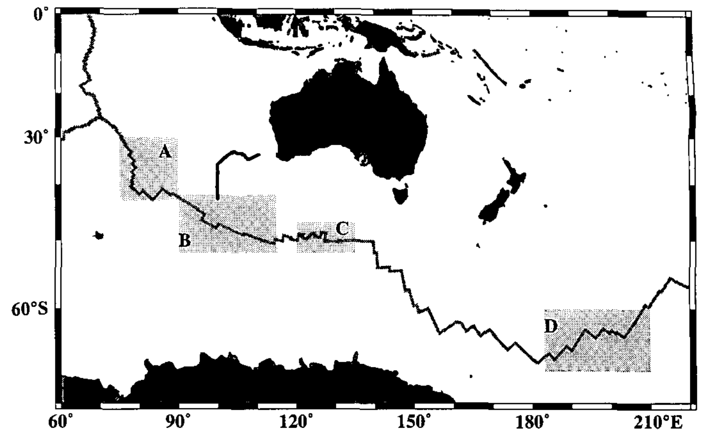

Figure 3. Index map for areas considered in this study. Thick gray line marks mid-ocean ridge system. Shaded boxes show locations of maps in Figure 5.

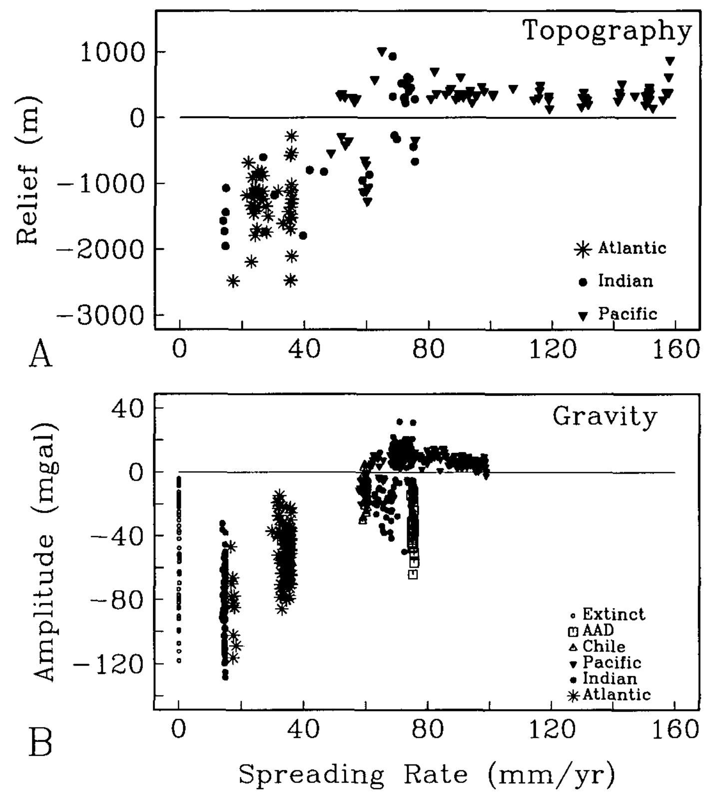

Figure 4. Variation of ridge-axis morphology and gravity anomaly with spreading rate. A: Axial topographic relief vs. spreading rate from Small (1993). B: Axial gravity-anomaly amplitude measured at 646 locations on ridges south of lat 30°S. Note coincident change in polarity and rate dependence between 60 and 80 mm/yr.

tain significant errors (~5 mgal) associated with poor navigation and unmodeled turns. It is known that high-quality shipboard gravity measurements generally have greater spatial resolution than satellite gravity measurements (Small and Sandwell, 1992; Neumann et al., 1993) so in this study we use the shipboard data as ground truth. The resolution of the satellite data for different wavelength anomalies is given by the spectral coherence (Bendat and Piersol, 1986); high coherence (>0.5) indicates good agreement between the two data sets. The satellite and shipboard data both accurately resolve anomalies with wavelengths longer than ~35 km but become increasingly incoherent at shorter wavelengths (<25 km) (Fig. 2B). If half-wavelengths as short as 13 km can be accurately resolved, then the gravity anomaly of a small axial rise should be recoverable, and the broader, larger amplitude axial-valley anomaly should be easily recognized in the satellite data (see Fig. 5).

SPREADING RATE DEPENDENCE

The remote locations of most intermediate-spreading-rate ridges on the primary ridge system (Fig. 3) have so far precluded a thorough understanding of the factors controlling axial morphology. In a survey of the morphology and tectonics of the Mid-Atlantic Ridge, Macdonald (1986) compiled estimates of axial-valley relief on several ridges and concluded that the axial valley disappears gradually, at spreading rates between 50 and 90 mm/yr.

More detailed analyses of available underway bathymetry data and satellite altimeter profile data have indicated that transitions from slow- to fast-spreading ridge axis morphology occur in a fairly narrow range of intermediate spreading rates. In a global study of ridge-axis gravity anomalies using Geosat Exact Repeat Mission profiles, we found that gravity anomaly amplitude decreases with increasing spreading rate on slow-spreading ridges, whereas anomaly amplitude remains relatively constant on fast-spreading ridges Small and Sandwell (1989). The transition from rate dependence to rate independence coincides with a polarity transition from the gravity lows characteristic of slow-spreading ridges to gravity highs seen at fast-spreading ridges. The satellite coverage now available allows us to determine more accurately the location of the ridge axis,

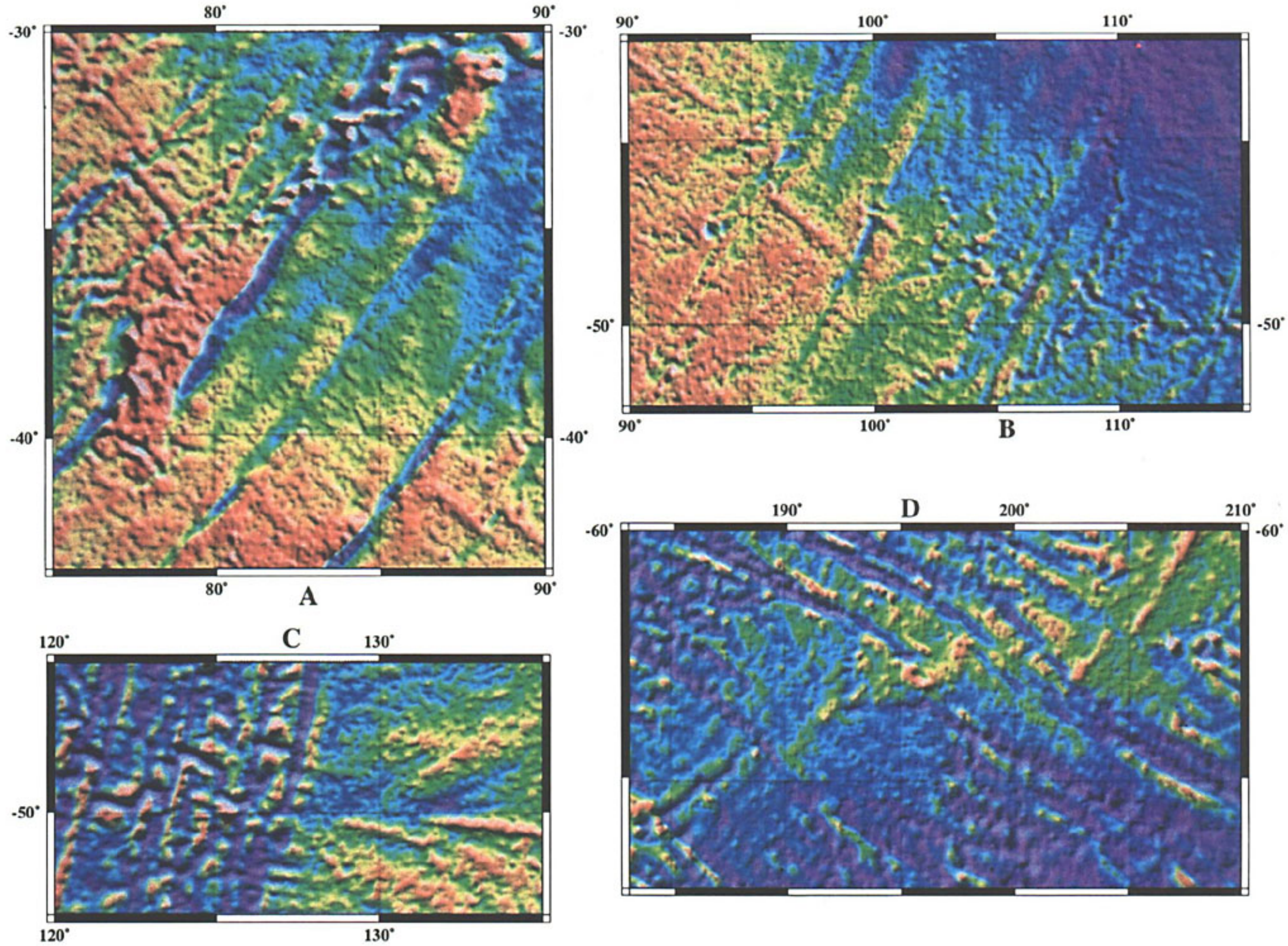

Figure 5. Examples of ridge-axis transitions on ridges in southern oceans. Each satellite gravity map shows anomaly amplitude ranging from −20 mgal (purple) to 20 mgal (red). In each region ridge axis changes from linear gravity high, characteristic of fast-spreading ridges, to linear low with flanking highs, typical of slow-spreading ridges. Spreading-rate ranges are (A) 62–72 mm/yr, (B) 72–75 mm/yr, (C) 73–75 mm/yr, and (D) 56–72 mm/yr.

thereby greatly reducing the chance of errors in estimates of the location and polarity of the axial anomaly.

Although the marine gravity field is affected by seafloor density variations and subseafloor structure, at short wavelengths ($\lambda < \sim 100$ km) it is controlled by seafloor morphology (Cochran, 1979). For this reason, changes in the nature of the ridge-axis gravity anomaly are assumed to correspond to changes in the morphology. Detailed global studies of available ridge-axis bathymetry profiles by Small (1993) and Malinverno (1993) support our previous findings (Small and Sandwell, 1989) (Fig. 4A).

The spatial coverage offered by the recently declassified satellite gravity data is a significant improvement over the previously available distribution of ship tracks and widely spaced satellite tracks. To give a more complete picture of the nature of the transition from slow- to fast-spreading structure, 646 ridge-perpendicular gravity profiles have been analyzed along the entire ridge system south of 30°S. The method described by Small (1993) was used to measure peak to trough amplitudes for axial gravity anomalies (Fig. 4B). As in previous studies we find a transition in the polarity and rate dependence of the ridge-axis anomalies at spreading rates between 60 and 80 mm/yr. The coverage offered by the satellite data gives us a significant advantage over previous studies and provides not only a continuous set of profiles for every ridge segment in the study area but also a more detailed knowledge of the location of the ridge axis than was previously available.

INTERMEDIATE-RATE TRANSITIONS

Satellite gravity maps provide the first detailed look at the nature of intermediate-spreading-rate transitions in the southern oceans (Fig. 5). Although the smaller ridge-axis anomalies are near the limit of the resolution for the satellite gravity data, it is apparent from Figure 5 that the anomalies are generally well resolved and that the characteristics of fast- and slow-spreading ridges can be distinguished. In these images the axial valleys, characteristic of slow-spreading ridges, are indicated by linear gravity lows flanked on either side by gravity highs. Axial ridges, characteristic of fast-spreading ridges, are shown by smaller amplitude, linear gravity highs. A SeaMARC II survey of the region shown in Figure 5C (Palmer et al., 1993) supports these interpretations.

Although these transitions from slow- to fast-spreading-rate structure occur within a narrow range of spreading rates, Figure 5 indicates that it may not always be spatially abrupt. In most cases there appears to be a small region, between the well-defined axial high and axial low, where a ridge-axis anomaly is not apparent. The absence of abrupt spatial transitions in the gravity data may accurately reflect the nature of the seafloor morphology in these areas, or it may result from the limited resolution of the satellite altimeter.

It is apparent that the transition from slow- to fast-spreading structure is not controlled by spreading rate alone. Well-known exceptions to the patterns shown in Figure 4 exist on the slow-spreading Reykjanes Ridge and in the faster spreading Australian-Antarctic Discordance. The Southeast Indian Ridge contains several potential transition areas that all have essentially the same spreading rate (70–75 mm/yr). It seems likely that the thermal structure at the ridge axis, which is controlled primarily by spreading rate, would exert the ultimate control on the morphology. Phipps Morgan and Chen (1993) discussed in greater detail the importance of thermal structure and crustal thickness on ridge-axis morphology. At a single spreading rate, local temperature variations may be considered perturbations to the large-scale thermal structure, which is controlled by spreading rate. This would suggest that ridge-axis morphology is controlled by a threshold phenomenon that is sensitive to relatively small changes in temperature (Small and Sandwell, 1989). A possible candidate for such a threshold mechanism was proposed by Chen and Morgan (1990), but more detailed surveys of transitions will be necessary to test their model.

A factor influencing the nature of the transitions may be the proximity of hot spots and the availability of melt at the ridge axis. Asthenosphere produced at nearby hot spots may be channeled to the ridge, as proposed by Vogt and Johnson (1975), where it may affect the process of crustal accretion, indirectly controlling the axial morphology. Royer and Schlich (1988) discussed the influence of the Amsterdam–St. Paul hot spot on the ridge axis in the immediate vicinity of the hot spot. Lava dredged from the ridge axis in this area have been shown to be geochemically related to both the Amsterdam–St Paul and Kerguelen hot spots (Michard et al., 1986). If asthenosphere migrates to the axis of the Southeast Indian Ridge along the unnamed fracture zone that intersects the axis near long 86°E, then it may contribute to the robust axial gravity high seen to the east of the fracture zone. Similar arguments may be made for the shrinking and eventual disappearance of the axial high on the Pacific Antarctic Rise south of the Louisville hot spot (Fig. 5D). The axial gravity anomaly also changes near the Bouvet Triple Junction on the Mid-Atlantic Ridge, although a typical fast-spreading anomaly never develops. An understanding of the transitions will require detailed surveys of these areas, for which the satellite gravity data will be an important reconnaissance tool.

CONCLUSIONS

Gravity maps derived from satellite data provide the first detailed look at many mid-ocean ridges in the southern oceans. The satellite gravity measurements used in this study accurately resolve features with half-wavelengths longer than 13 km, thereby allowing the location of the ridge axis to be mapped in much greater detail than was previously possible. Amplitude and polarity measurements of ridge-axis gravity anomalies in the southern oceans agree with results of previous studies that showed a transition from spreading-rate-dependent structure to rate independence at intermediate spreading rates (60–80 mm/yr). Examples of these transitions are seen on the Southeast Indian Ridge and the Pacific Antarctic Ridge. Although geophysical and petrologic data are sparse in these transitional areas, we believe that the morphology is controlled by thermal structure, which may be strongly influenced by asthenosphere derived from nearby hot spots.

REFERENCES CITED

Bendat, J.S., and Piersol, A.G., 1986, Random data, analysis and measurement procedures (second edition): New York, John Wiley & Sons.

Chen, Y., and Morgan, W.J., 1990, Rift valley/no rift valley transition at mid-ocean ridges: Journal of Geophysical Research, v. 95, p. 17,571–17,583.

Cochran, J.R., 1979, An analysis of isostasy in the world's oceans: 2, Mid-ocean ridge crests: Journal of Geophysical Research, v. 84, p. 4713–4729.

Haxby, W.F., Karner, G.D., LaBrecque, J.L., and Weissel, J.K., 1983, Digital images of combined continental and oceanic data sets and their use in tectonic studies: Eos (Transactions, American Geophysical Union), v. 64, p. 995–1004.

Heezen, B.C., 1960, The rift in the ocean floor: Scientific American, v. 203, p. 99–110.

Lonsdale, P., 1989, Segmentation of the Pacific Nazca spreading center, 1°N–20°S: Journal of Geophysical Research, v. 94, p. 12,197–12,225.

Macdonald, K.C., 1986, The crest of the Mid Atlantic Ridge: Models for crustal generation and tectonics, *in* Vogt, P.R., ed., The western North Atlantic region: Boulder, Colorado, Geological Society of America, Geology of North America, v. M, p. 51–68.

Malinverno, A., 1993, Transition between a valley and a high at the axis of mid-ocean ridges: Geology, v. 21, p. 639–642.

Menard, H.W., 1960, The East Pacific Rise: Science, v. 132, p. 1737–1746.

Michard, A., Montigny, R., and Schlich, R., 1986, Geochemistry of the mantle beneath the Rodriguez triple junction and Southeast Indian Ridge: Earth and Planetary Science Letters, v. 78, p. 104–114.

Neumann, G.A., Forsyth, D.W., and Sandwell, D.T., 1993, Comparison of marine gravity from shipboard and high-density satellite altimetry along the Mid-Atlantic Ridge, 30.5°–35.5°S: Geophysical Research Letters, v. 20, p. 1639–1642.

Palmer, J., Sempère, J.C., Christie, D.M., Phipps Morgan, J., 1993, Morphology and tectonics of the Australian-Antarctic discordance between 123°E and 128°E: Marine Geophysical Researches, v. 15, p. 121–152.

Phipps Morgan, J., and Chen, Y.J., 1993, The genesis of oceanic crust: Magma injection, hydrothermal circulation, and crustal flow: Journal of Geophysical Research, v. 98.

Rapp, R.H., 1983, The determination of geoid undulations and gravity anomalies from Seasat altimeter data: Journal of Geophysical Research, v. 88, p. 1552–1562.

Royer, J.Y., and Schlich, R., 1988, Southeast Indian Ridge between the Rodriguez triple junction and the Amsterdam and St. Paul islands: Detailed kinematics for the past 20 m.y.: Journal of Geophysical Research, v. 93, p. 13,524–13,550.

Sandwell, D.T., 1992, Antarctic marine gravity from high density satellite altimetry: Geophysical Journal International, v. 109, p. 437–448.

Small, C., 1993, A quantitative analysis of mid-ocean ridge axial topography: Geophysical Journal International.

Small, C., and Sandwell, D.T., 1989, An abrupt change in ridge axis gravity with spreading rate: Journal of Geophysical Research, v. 94, p. 17,383–17,392.

Small, C., and Sandwell, D.T., 1992, A comparison of satellite and shipboard gravity measurements in the Gulf of Mexico: Geophysics, v. 57, p. 885–893.

Vogt, P.R., and Johnson, G.L., 1975, Transform faults and longitudinal flow below the midoceanic ridge: Journal of Geophysical Research, v. 80, p. 1399–1428.

Manuscript received August 4, 1993
Revised manuscript received November 9, 1993
Manuscript accepted November 22, 1993